



This is a repository copy of *Vehicle to Vehicle Charging (V2V) Bases on Wireless Power Transfer Technology*.

White Rose Research Online URL for this paper:
<http://eprints.whiterose.ac.uk/141968/>

Version: Accepted Version

Proceedings Paper:

Mou, X., Zhao, R. and Gladwin, D.T. (2018) Vehicle to Vehicle Charging (V2V) Bases on Wireless Power Transfer Technology. In: IECON 2018 - 44th Annual Conference of the IEEE Industrial Electronics Society. IECON 2018 - 44th Annual Conference of the IEEE Industrial Electronics Society, 21-23 Oct 2018, Washington, DC, USA. IEEE , pp. 4862-4867. ISBN 978-1-5090-6684-1

<https://doi.org/10.1109/iecon.2018.8592888>

© 2018 IEEE. Personal use of this material is permitted. Permission from IEEE must be obtained for all other users, including reprinting/ republishing this material for advertising or promotional purposes, creating new collective works for resale or redistribution to servers or lists, or reuse of any copyrighted components of this work in other works. Reproduced in accordance with the publisher's self-archiving policy.

Reuse

Items deposited in White Rose Research Online are protected by copyright, with all rights reserved unless indicated otherwise. They may be downloaded and/or printed for private study, or other acts as permitted by national copyright laws. The publisher or other rights holders may allow further reproduction and re-use of the full text version. This is indicated by the licence information on the White Rose Research Online record for the item.

Takedown

If you consider content in White Rose Research Online to be in breach of UK law, please notify us by emailing eprints@whiterose.ac.uk including the URL of the record and the reason for the withdrawal request.



eprints@whiterose.ac.uk
<https://eprints.whiterose.ac.uk/>

Vehicle to Vehicle Charging (V2V) Bases on Wireless Power Transfer Technology

Xiaolin Mou

Department of Electronic and
Electrical Engineering
University of Sheffield, UK
Email: x.mou@sheffield.ac.uk

Rui Zhao

Department of Electronic and
Electrical Engineering
University of Sheffield, UK
Email: r.zhao@sheffield.ac.uk

Daniel Gladwin

Department of Electronic and
Electrical Engineering
University of Sheffield, UK
Email: d.gladwin@sheffield.ac.uk

Abstract—The slow development of energy storage technology combined with a limited number of plug-in charging stations negatively affects people’s desire to purchase pure battery electric vehicles. A new wireless vehicle-to-vehicle charging technology structure is proposed, which can function with plug-in electric vehicles or operate independently. With a limited number of charging stations this technology can be used to increase charging opportunities through vehicle-to-vehicle (V2V) charging. V2V charging requires a number of technical challenges to be overcome including the angular offset of the wireless power transfer resonant coils. The mutual inductance between two resonant coils is a key parameter for high power and efficient transfer of power. This paper presents the theory of angular offset multi-turn coil design.

Index Terms—Vehicle to Vehicle Charging, Wireless Power Transfer, Angular Offset, Coil Design

I. INTRODUCTION

Demand for renewable energy generation and electric vehicles (EVs) has increased in recent years due to growing concerns over climate change, air pollution and energy security [1]. Car companies have been developing various types of EVs such as pure battery EVs, hybrid EVs *etc.*. Hybrid EVs are the most popular in worldwide markets among all EVs. However, the slow development of electricity storage technology is a key issue for EVs’ development. The electricity storage of EVs is complex to design due to the EVs battery needing high energy density, affordable cost, long cycle life time, good safety, reliability and many other requirements. Currently, most EVs use plug-in charging technology. However, there are various downsides associated with plug-in charging such as the charging cables on the floor creating a potential trip hazard; the inconvenience to the user of having to physically plug-in/unplug the charger, particularly in bad weather; the degradation of the charger cables over time can lead to leakage, and a potential hazard for the user [2]. Wireless charging for EVs can help to solve these problems.

A regulatory and consumer-led insistence on greater levels of safety and convenience has prompted an evergrowing demand for wireless power transfer (WPT). In 2012 automakers first announced their plans to include wireless charging technology on future EVs. In 2014, Plugless Power began offering WPT kits for the Chevy Volt, Nissan LEAF, and Cadillac ELR. In the years since, Plugless has expanded its offering

to include the BMW i3, Mercedes S550e, and Tesla Model S [3]. Currently, the most common form of design of wireless charging technology for EVs includes a transmitter coil, which is embedded in the floor of the charging area, and a receiver coil which is embedded in the car’s chassis. The transmitter coil connects to the power supply (grid or storage), and the receiver coil connects to the car’s battery.

Although the government has issued many different incentives to encourage people to buy electric cars, many consumers are still reluctant to purchase pure battery EVs. There are a number of causes for this trepidation, key amongst them is anxiety over the need to recharge the vehicle during a journey. The number of plug-in charging stations is limited and may not be located at a convenient site in relation to their route, as compared to the convenience and ease of locating a petrol station. A further issue may then arise for the user having located a charging station, finding that the designated charging slots are already taken by other vehicles. This paper proposes a new structure of wireless charging technology for EVs called wireless vehicle-to-vehicle (V2V) charging which can work together with plug-in charge EVs or operate independently. The transmitter coil and the receiver coil are embedded in the front and rear of the car, respectively. This structure can effectively solve the issue of the limited number of plug-in stations. Additionally, a car with V2V technology can also achieve auxiliary charging between moving vehicles, thus reducing the need to locate a fixed charging station. Section II introduces the structure of wireless V2V charging system. Section III proposes the fundamental theory of angular offset multi-turn coil design. Section IV discusses the results of the simulation. Finally is the conclusion.

II. STRUCTURE OF WIRELESS VEHICLE TO VEHICLE (V2V) CHARGING SYSTEM

The proposed V2V system is primarily designed for two applicable scenarios : one is plug-in EVs charging through a wireless V2V charging integration system, as shown in Fig. 1. Another is called the vehicle assistance system, as shown in Fig. 2.

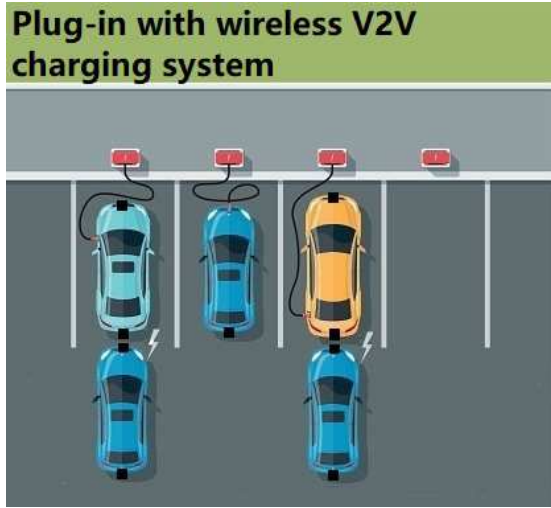


Fig. 1: Plug-in with wireless V2V charging system

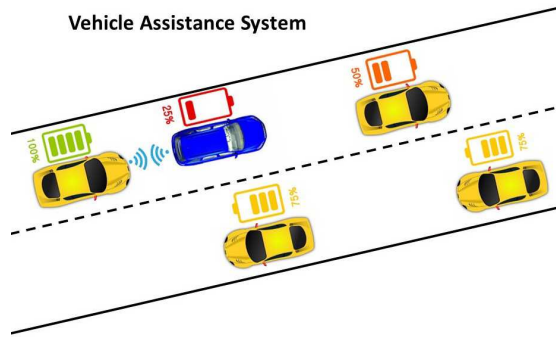


Fig. 2: Vehicle Assistance System bases on wireless charging

A. Plug-in with wireless V2V charging system

At present, the biggest drawback of plug-in charging systems is the limited number of charging stations. In addition, charging stations require regular maintenance and service to ensure the equipment is working properly. The plug-in with wireless V2V charging system can help to solve the above issues. Fig. 1 shows the structure of the system. The transmitter coil and receiver coil are embedded in the front and rear of the car. The first car can automatically charge wirelessly to the car behind it.

B. Vehicle Assistance wireless charging system

Fig. 2 shows the vehicle assistance charging system. When the vehicle's battery runs low, the driver can request the help of other EVs on the road to wirelessly charge the vehicle. In this process, there are several auxiliary technologies, such as vehicle-to-vehicle communication, GPS, and battery state of charge detection *etc.*. The driver can find suitable vehicles using an application on their smart device that indicates available donor vehicle energy, pricing, distance, and other factors. This concept can reduce the potential EV buyers'

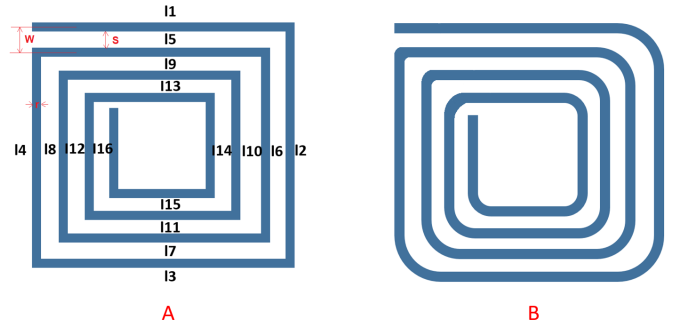


Fig. 3: Coil design for wireless V2V charging system

anxiety that an EV battery will run flat some distance from the nearest charging station.

The magnetic resonant coupling WPT technology is a good choice for wireless V2V charging due to its high power transfer efficiency with long transmitting distance. Compared with the common wireless magnetic resonant coupling EV charging technologies, the proposed wireless V2V charging system not only has lateral offset but, because of the location of the resonant coils, also angular offset. The next section will focus on introducing the angular offset multi-turn coil design.

III. FUNDAMENTAL THEORY OF ANGULAR OFFSET MULTI-TURN COIL DESIGN

C.Cai *et al.* [4] proposes that compared with a circular coil, the mutual inductance of a square coil has greater stability and changes more slowly when a horizontal offset occurs. However, the current at the right angle of a square coil is uneven due to skin effect and proximity effect; a fillet design can be adopted to avoid the effect at the corner of a square coil to reduce resistance losses. In order to simplify the mathematical calculations, the right angle of a square coil (Fig. 3 A) is chosen to do the analysis in this paper, and corner angle of a square coil (Fig. 3 B) is used in hardware implementation.

A. The parameters of multi-turns coil

Fig. 3(A) shows the square coil design for the wireless V2V charging system, where r is the diameter of the conductor; s is the space between two adjacent conductors; $w = s + r$ is distance of track centres between two adjacent conductors. The main parameters of the coil include capacitance C , inductance L , and resistance R .

1) *Capacitance*: The capacitance C is determined by the inductance of coil L and the resonant frequency f :

$$C = \frac{1}{(2f\pi)^2 L} \quad (1)$$

2) *Inductance*: The total inductance L of the coil is equal to the sum of self-inductance L_S of each straight segment conductor plus all the mutual inductances L_M between these segments. The mutual inductance between the straight segment conductors L_M divided into positive mutual inductance L_{M+}

and negative mutual inductance L_{M-} . The positive mutual inductance is the mutual inductance between conductors that have the same current direction. The negative mutual inductance is the mutual inductance between conductors that have the opposite current direction. The total inductance L of the coil can be indicated as:

$$L = L_S - L_{M+} - L_{M-} \quad (2)$$

The self-inductance of the straight segment conductor L_{S_i} [5]:

$$L_{S_i} = 0.02 \cdot l \cdot \left\{ \ln\left(\frac{l}{r}\right) + 0.50049 + \frac{2r}{3l} \right\} \quad (3)$$

where l is the length of conductor (each straight segment of the coil), r is the diameter of the conductor. Fig. 3 A shows a four-turn spiral coil, so the total self-inductance of the coil is $L_S = L_{S1} + L_{S2} + L_{S3} + \dots + L_{S16}$.

The mutual inductance of the straight segment conductors L_{M_i} [5]:

$$L_{M_i} = 2 \cdot l \cdot F \quad (4)$$

where l is the length of straight segment conductor, F is the mutual inductance parameter and calculated as [5]:

$$F = \ln\left\{\left(\frac{l}{d}\right) + \left[1 + \left(\frac{l}{d}\right)^2\right]^{\frac{1}{2}}\right\} - \left[1 + \left(\frac{d}{l}\right)^2\right]^{\frac{1}{2}} + \left(\frac{d}{l}\right) \quad (5)$$

where d is the distance between two conductors.

The mutual inductance between two conductors calculation method is shown in Fig. 4. j, k are indications of conductors, and p, q are indications of the difference in length between two conductors.

$$M_{j,k} = \frac{1}{2} \left\{ (M_{k+p} + M_{k+q}) - (M_p + M_q) \right\} \quad (6)$$

The mutual inductance of conductors is maximized if the two segments are in parallel, and minimum if they are placed in orthogonal (90 degree) topology. So for the four-turn spiral coil:

The positive mutual inductance:

$$\begin{aligned} L_{M+} = & 2(L_{M_{1,5}} + L_{M_{1,9}} + L_{M_{1,13}}) + \\ & 2(L_{M_{5,9}} + L_{M_{5,13}}) + L_{2(M_{9,13})} + \\ & 2(L_{M_{3,7}} + L_{M_{3,11}} + L_{M_{3,15}}) + \\ & 2(L_{M_{7,11}} + L_{M_{7,15}}) + 2(L_{M_{11,15}}) + \\ & 2(L_{M_{2,6}} + L_{M_{2,10}} + L_{M_{2,14}}) + \\ & 2(L_{M_{6,10}} + L_{M_{6,14}}) + 2(L_{M_{10,14}}) + \\ & 2(L_{M_{4,8}} + L_{M_{4,12}} + L_{M_{4,16}}) + \\ & 2(L_{M_{8,12}} + L_{M_{8,16}}) + 2(L_{M_{12,16}}) \end{aligned} \quad (7)$$

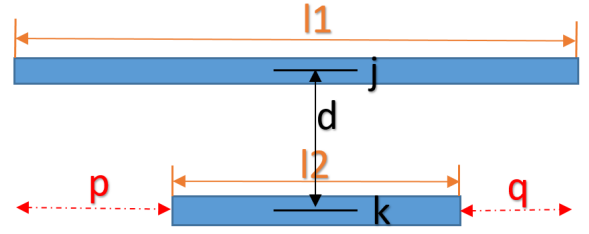


Fig. 4: Diagram of mutual inductance between two conductors

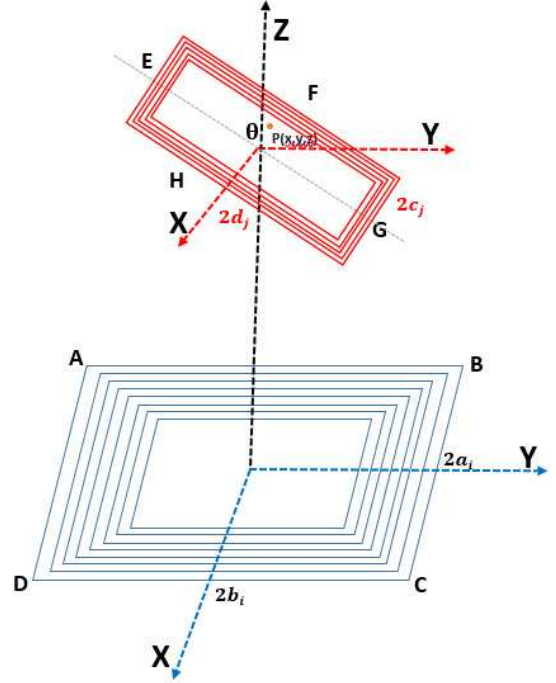


Fig. 5: Diagram of wireless V2V charging system

The negative mutual inductance:

$$\begin{aligned} L_{M-} = & 2(L_{M_{1,3}} + L_{M_{1,7}} + L_{M_{1,11}} + L_{M_{1,15}}) + \\ & 2(L_{M_{5,3}} + L_{M_{5,7}} + L_{M_{5,11}} + L_{M_{5,15}}) + \\ & 2(L_{M_{9,3}} + L_{M_{9,7}} + L_{M_{9,11}} + L_{M_{9,15}}) + \\ & 2(L_{M_{13,3}} + L_{M_{13,7}} + L_{M_{13,11}} + L_{M_{13,15}}) + \\ & 2(L_{M_{2,4}} + L_{M_{2,8}} + L_{M_{2,12}} + L_{M_{2,16}}) + \\ & 2(L_{M_{6,4}} + L_{M_{6,8}} + L_{M_{6,12}} + L_{M_{6,16}}) + \\ & 2(L_{M_{10,4}} + L_{M_{10,8}} + L_{M_{10,12}} + L_{M_{10,16}}) + \\ & 2(L_{M_{14,4}} + L_{M_{14,8}} + L_{M_{14,12}} + L_{M_{14,16}}) \end{aligned} \quad (8)$$

B. The mutual inductance between transmitter coil and receiver coil with angular offset

Fig. 5 shows the diagram of two multi-turn resonant coils with angular offset. ABCD is the multi-turn transmitter coil

and EFGH is the multi-turn receiver coil. a_i , b_i indicate the weight and the length of transmitter coil, respectively. c_j , d_j indicate the weight and the length of receiver coil, respectively. i and j are the turns of the coils, assuming the coil parameters like Fig. 3, r is the diameter of the conductor; s is the space between two adjacent conductors; $w = s + r$ is the distance of track centres between two adjacent conductors, a_i is equal to $a_1 - (i - 1)w$. θ is the angular offset between transmitter coil and receiver coil. $P_{(x,y,z)}$ is arbitrary point in receiver coil. Here we only use side segment AB as an example to explain the calculation method, the calculation for the other sides uses the same method.

The magnetic flux density B in side segment AB can be expressed as [6] :

$$B_{AB_x} = \frac{\mu_0}{4\pi} \cdot \frac{-1}{(a_i + x)^2 + z^2} \cdot \left[\frac{b_i + y}{\sqrt{(a_i + x)^2 + z^2 + (b_i + y)^2}} + \frac{b_i - y}{\sqrt{(a_i + x)^2 + z^2 + (b_i - y)^2}} \right] \quad (9)$$

$$B_{AB_z} = \frac{\mu_0}{4\pi} \cdot \frac{a_i + x}{(a_i + x)^2 + z^2} \cdot \left[\frac{b_i + y}{\sqrt{(a_i + x)^2 + z^2 + (b_i + y)^2}} + \frac{b_i - y}{\sqrt{(a_i + x)^2 + z^2 + (b_i - y)^2}} \right] \quad (10)$$

where μ_0 is the permeability of free space. The y-directed magnetic fields caused by segment BC and DA are not affected by the mutual inductance because of the dot product between the normal vector of the receiver coil and the y-directed fields being zero. So the magnetic flux density B of segment BC and DA only has z-directed fields.

The magnetic flux ϕ can be calculated as [7]:

$$\phi_{AB_x} = \int_{-d_j}^{d_j} \int_{-c_j}^{c_j} -\cos(\theta) \cdot B_{AB_x} d_y d_x \quad (11)$$

$$\phi_{AB_z} = \int_{-d_j}^{d_j} \int_{-c_j}^{c_j} \sin(\theta) \cdot B_{AB_z} d_y d_x \quad (12)$$

The first integral result in ϕ_{AB_x} and ϕ_{AB_z} :

$$\phi_{AB_x(1)} = \frac{\cos(\theta)\mu_0}{2\pi} \cdot \int_{-c_j}^{c_j} \frac{1}{(a_i + x)^2 + z^2} \cdot (\sqrt{(a_i + x)^2 + z^2 + (b_i + d_j)^2} - \sqrt{(a_i + x)^2 + z^2 + (b_i - d_j)^2}) d_x \quad (13)$$

$$\phi_{AB_z(1)} = \frac{\sin(\theta)\mu_0}{2\pi} \cdot \int_{-c_j}^{c_j} \frac{a_i + x}{(a_i + x)^2 + z^2} \cdot (\sqrt{(a_i + x)^2 + z^2 + (b_i + d_j)^2} - \sqrt{(a_i + x)^2 + z^2 + (b_i - d_j)^2}) d_x \quad (14)$$

By substituting $a_i + x = x'$ The second integral in $\phi_{AB_x(1)}$ and $\phi_{AB_z(1)}$ becomes:

$$\phi_{AB_x(2)} = \frac{\cos(\theta)\mu_0}{2\pi} \cdot \int_{a_i - c_j}^{a_i + c_j} \frac{1}{(x')^2 + z^2} \cdot (\sqrt{(x')^2 + z^2 + (b_i + d_j)^2} - \sqrt{(x')^2 + z^2 + (b_i - d_j)^2}) d_{x'} \quad (15)$$

$$\phi_{AB_z(2)} = \frac{\sin(\theta)\mu_0}{2\pi} \cdot \int_{a_i - c_j}^{a_i + c_j} \frac{x'}{(x')^2 + z^2} \cdot (\sqrt{(x')^2 + z^2 + (b_i + d_j)^2} - \sqrt{(x')^2 + z^2 + (b_i - d_j)^2}) d_{x'} \quad (16)$$

The type integration can be calculated using:

$$\int \frac{1}{x^2 + z^2} \sqrt{x^2 + z^2 + m^2} d_x = \log(\sqrt{x^2 + z^2 + m^2} + x) + \frac{m}{z} \tan^{-1}\left(\frac{mx}{z\sqrt{x^2 + z^2 + m^2}}\right) + C \quad (17)$$

$$\int \frac{x}{x^2 + z^2} \sqrt{x^2 + z^2 + m^2} d_x = \sqrt{x^2 + z^2 + m^2} - m \cdot \arctan^{-1}\left(\frac{m}{\sqrt{x^2 + z^2 + m^2}}\right) + C \quad (18)$$

The second integral result of ϕ_{AB_x} and ϕ_{AB_z} :

$$\begin{aligned} \phi_{AB_x} = & \frac{\cos(\theta)\mu_0}{2\pi} \cdot \\ & \left[\log(\sqrt{(a_i + c_j)^2 + z^2 + (b_i + d_j)^2} + (a_i + c_j)) + \frac{b_i + d_j}{z} \cdot \arctan\left(\frac{(b_i + d_j) \cdot (a_i + c_j)}{z \cdot \sqrt{(a_i + c_j)^2 + z^2 + (b_i + d_j)^2}}\right) \right. \\ & - \log(\sqrt{(a_i + c_j)^2 + z^2 + (b_i - d_j)^2} + (a_i + c_j)) - \frac{b_i - d_j}{z} \cdot \arctan\left(\frac{(b_i - d_j) \cdot (a_i + c_j)}{z \cdot \sqrt{(a_i + c_j)^2 + z^2 + (b_i - d_j)^2}}\right) \\ & - \log(\sqrt{(a_i - c_j)^2 + z^2 + (b_i + d_j)^2} + (a_i - c_j)) + \frac{b_i + d_j}{z} \cdot \arctan\left(\frac{(b_i + d_j) \cdot (a_i - c_j)}{z \cdot \sqrt{(a_i - c_j)^2 + z^2 + (b_i + d_j)^2}}\right) \\ & \left. + \log(\sqrt{(a_i - c_j)^2 + z^2 + (b_i - d_j)^2} + (a_i - c_j)) + \frac{b_i - d_j}{z} \cdot \arctan\left(\frac{(b_i - d_j) \cdot (a_i - c_j)}{z \cdot \sqrt{(a_i - c_j)^2 + z^2 + (b_i - d_j)^2}}\right) \right] \quad (19) \end{aligned}$$

$$\begin{aligned}
\phi_{ABz} &= \frac{\sin(\theta)\mu_0}{2\pi} \cdot \\
&[\sqrt{(a_i + c_j)^2 + z^2 + (b_i + d_j)^2} - \\
&(b_i + d_j) \cdot \arctan^{-1}\left(\frac{(b_i + d_j)}{\sqrt{(a_i + c_j)^2 + z^2 + (b_i + d_j)^2}}\right) \\
&- \sqrt{(a_i + c_j)^2 + z^2 + (b_i - d_j)^2} + \\
&(b_i - d_j) \cdot \arctan^{-1}\left(\frac{(b_i - d_j)}{\sqrt{(a_i + c_j)^2 + z^2 + (b_i - d_j)^2}}\right) \quad (20) \\
&- \sqrt{(a_i - c_j)^2 + z^2 + (b_i + d_j)^2} + \\
&(b_i + d_j) \cdot \arctan^{-1}\left(\frac{(b_i + d_j)}{\sqrt{(a_i - c_j)^2 + z^2 + (b_i + d_j)^2}}\right) \\
&+ \sqrt{(a_i - c_j)^2 + z^2 + (b_i - d_j)^2} - \\
&(b_i - d_j) \cdot \arctan^{-1}\left(\frac{(b_i - d_j)}{\sqrt{(a_i - c_j)^2 + z^2 + (b_i - d_j)^2}}\right)]
\end{aligned}$$

The magnetic flux ϕ produced by the other three segments (BC,CD,DA) can be calculated in the same method like the segment AB. The total magnetic flux by the i th coil with unit current is $\phi_{ij} = \phi_{X_{AB}} + \phi_{X_{CD}} + \phi_{Z_{AB}} + \phi_{Z_{BC}} + \phi_{Z_{CD}} + \phi_{Z_{DA}}$, and the mutual inductance between the i th coil with the j th coil is M_{ij} , $M_{ij} = \phi_{ij}$. If the numbers of the turns of transmitter coil and receiver coil are $N1$ and $N2$, respectively, the total mutual inductance M is:

$$M = \sum_{i=1}^{N1} \sum_{j=1}^{N2} M_{ij} \quad (21)$$

C. The power transfer efficiency of V2V wireless charging system

The PTE η can be defined as [8]:

$$\eta = \frac{\sqrt{1 + \frac{K^2}{L_T L_R}} - 1}{\sqrt{1 + \frac{K^2}{L_T L_R}} + 1} \quad (22)$$

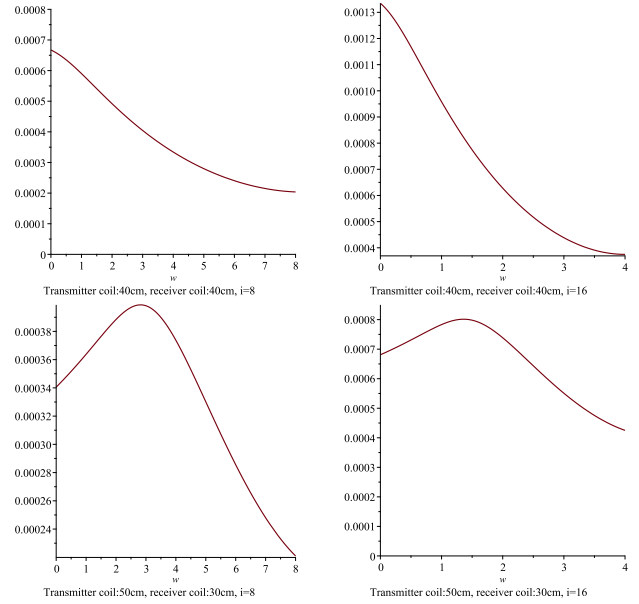
where L_T and L_R are the inductance of the transmitter coil and the receiver coil, respectively. $K = \frac{M\omega}{2\sqrt{L_T L_R}}$ is the coupling coefficient between the two resonant coils. ω is the resonant frequency and M is the mutual inductance.

Simultaneous equations (19) (20) (21) (22), can get the efficiency of the multi-turn coils magnetic resonant WPT system with angular offset.

IV. RESULT

The mutual inductance M between two resonant coils is an important parameter in wireless magnetic resonant coupling charge technology. According to the above equations, the space between the two adjacent conductors w , and the number of turns in the coil i , can affect the mutual inductance M .

Assuming that the transmitter coil and the receiver coil have the same number of turns. Fig. 6(a) shows the eight-turn coils design. The figure above shows that when the



(a) Eight-turn Coils

(b) Sixteen-turn Coils

Fig. 6: The relation between the mutual inductance M and the space between two adjacent conductors w

transmitter coil and the receiver coil are the same size, a high mutual inductance can be obtained when the spacing between two adjacent conductors w is zero. This means that when the transmitter coil and the receiver coil have the same specifications, the coils are closely wound to obtain a high mutual inductance. The figure below shows the lengths of the transmitter coil and the receiver coil are 50cm and 30cm, respectively. The distance between the two adjacent conductors w is about 3cm, and can achieve high mutual inductance. Compared with the fig. 6(b) sixteen-turn design, the results show that if the number of turns increases, the space between the adjacent conductors should decrease and a high mutual inductance can then be obtained. Moreover, the same size of transmitter coil and receiver coil is a good design.

V. CONCLUSION

This paper proposes a new structure of wireless V2V charging technology that can work together with plug-in EVs charging or operate independently. It can effectively solve the problem of a limited number of plug-in stations, and it can realize mutual power supply between vehicles. One issue with the wireless V2V charging technology is the angular offset due to the change in the location of the vehicle. Therefore, this paper presents the fundamental theory of multi-turn coil design with angular offset. Simulation results show that if the transmitter coil and receiver coil are the same size and closely wound, the system can achieve high mutual inductance. If the size of transmitter coil and the receiver coil are different, the coil will require an optimal design. In the future, we will focus

our attention onto the hardware implementation and design and build a model for this wireless V2V charging system.

REFERENCES

- [1] J. Traube, F. Lu, D. Maksimovic, J. Mossoba, M. Kromer, P. Faill, S. Katz, B. Borowy, S. Nichols, and L. Casey, "Mitigation of solar irradiance intermittency in photovoltaic power systems with integrated electric-vehicle charging functionality," *IEEE Transactions on Power Electronics*, vol. 28, no. 6, pp. 3058–3067, June 2013.
- [2] S. Li and C. C. Mi, "Wireless power transfer for electric vehicle applications," *IEEE Journal of Emerging and Selected Topics in Power Electronics*, vol. 3, no. 1, pp. 4–17, March 2015.
- [3] [Online]. Available: <https://www.fleetcarma.com>
- [4] C. Cai, J. Wang, Z. Fang, P. Zhang, M. Hu, J. Zhang, L. Li, and Z. Lin, "Design and optimization of load-independent magnetic resonant wireless charging system for electric vehicles," *IEEE Access*, vol. 6, pp. 17 264–17 274, 2018.
- [5] Y. Lee, "Antenna circuit design for rfid applications." [Online]. Available: <http://ww1.microchip.com/downloads/en/AppNotes/00710c.pdf>
- [6] J. Kim, H. C. Son, D. H. Kim, K. H. Kim, and Y. J. Park, "Efficiency of magnetic resonance wpt with two off-axis self-resonators," in *2011 IEEE MTT-S International Microwave Workshop Series on Innovative Wireless Power Transmission: Technologies, Systems, and Applications*, May 2011, pp. 127–130.
- [7] Y. Cheng and Y. Shu, "A new analytical calculation of the mutual inductance of the coaxial spiral rectangular coils," *IEEE Transactions on Magnetics*, vol. 50, no. 4, pp. 1–6, April 2014.
- [8] X. Mou, O. Groling, and H. Sun, "Energy-efficient and adaptive design for wireless power transfer in electric vehicles," *IEEE Transactions on Industrial Electronics*, vol. 64, no. 9, pp. 7250–7260, Sept 2017.